Synthesis of a Tethered Dibenzotetramethyltetraaza[14]annulene Macrocycle and The Di-nickel(II) Derivative

Journal:	*New Journal of Chemistry*
Manuscript ID	NJ-ART-06-2018-003154.R1
Article Type:	Paper
Date Submitted by the Author:	12-Sep-2018
Complete List of Authors:	Dey, Soumyajit; Temple University, Chemistry Dewey, Jacob; Temple University, Chemistry Wayland, Bradford; Temple University, Chemistry Zdilla, Michael; Temple University, Chemistry

NJC

ARTICLE

Synthesis of a Tethered Dibenzotetramethyltetraaza[14]annulene Macrocycle and The Di-nickel(II) Derivative

Received 00th January 20xx,
Accepted 00th January 20xx

DOI: 10.1039/x0xx00000x

www.rsc.org/

Soumyajit Dey, Jacob R. Dewey, Bradford B. Wayland*and Michael J. Zdilla*

Selective reaction of 2,6-isophthaloyl chloride at the methine positions of two dibenzotetramethyltetraaza[14]annulene (tmtaa) units results in tethering of the macrocycles by either one or two 2,6-isophthaloyl bridging groups. The single tethered dibenzotetramethyltetraaza[14]annulene derivative (SIT-tmtaa) was isolated and characterized by X-ray crystallography , ESI-MS, ^{1}H and ^{13}C NMR. The syn conformation of the two tmtaa units observed in the crystal structure, has tetraaza[14]annulene macrocycles that are more distorted from planarity than in the structure of the parent tmtaa. The di-nickel(II) complex was prepared and characterized by ESI-HRMS, ^{1}H and ^{13}C NMR. DFT computations place the LUMO on the 2,6-isophthaloyl bridge rather than on the tethered tmtaa units and suggest that the 2,6-isophthaloyl tether provides a level of flexibility in the inter tmtaa distances that is comparable to the Pacman Effect observed for tethered porphyrins. [Keywords: tmtaa, SIT-tmtaa and DIT-tmtaa]

Introduction

Tethering metal complexes is an effective approach for obtaining multiple metal sites in coordination complexes. A substantial effort has been directed to the design and preparation of tethered macrocycles with a wide variety of bridging spacer groups that have been applied in obtaining enhanced reaction rates and selectivity compared to complexes with a single metal site.[1-8] Chemical species that have multiple sites for substrate binding or reaction have been referred to as molecular tweezers.[7] The tethering of metallated π-ligands has implications for conformationally switchable molecules for various applications such as fluorescence.[9] There are numerous reports of tethered diporphyrin ligand systems (Fig. 1),[8] but there are no structurally characterized examples of tethered tetraaza[14]annulenes even though they are easily prepared and represent low cost N_4^{-2} macrocycle analogs of porphyrins.[2,10]

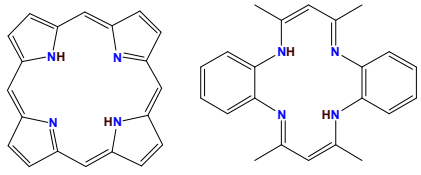

porphyrin tmtaa

Fig. 1 Structure of porphyrin and TMTAA.

Department of Chemistry, Temple University, 1901 N. 13th Street, Philadelphia, Pennsylvania 19122, United States.E-mail: mzdilla@temple.edu (M.J.Z.), E-mail: bwayland@temple.edu (B.B.W.).

Electronic Supplementary Information (ESI) available: [ESI-MS spectroscopic data, ^{13}C NMR spectra, cyclic voltammagrams, crystallographic Data and Data Collection Parameters, and details of density functional studies; crystallographic data is also available from the CCDC from deposition number 1850215. See DOI: 10.1039/x0xx00000x

Dibenzotetramethyltetraaza[14]annulene (tmtaa) and related derivatives bind metals as N_4^{2-} macrocycles in the same manner as porphyrins, but as non-planar, antiaromatic, 16-π-electron macrocycles. They differ electronically and structurally from the near planar aromatic 18-π-electron porphyrins. This article reports on using a 2,6-isophthaloyl bridging group in the facile preparation of the first structurally characterized covalently tethered ditetraaza[14]annulene ligand and on formation of the di-nickel(II) complex.

Results and Discussion

1. Design and Synthesis of a 2,6-Isophthaloyl Single Tethered Bis(Dibenzotetramethyltetraaza[14]Annulene (SIT-tmtaa):

Dibenzotetramethyltetraaza[14]annulene (tmtaa) (**1**) is known to react selectively with acid chlorides at the methine position to form carbonyl derivatives of tmtaa.[11] Reaction of tmtaa with the diacid chloride 2, 6-isophthaloyl was explored as a facile one-pot strategy to tether two tmtaa macrocycles together with a 2,6-isophthaloyl bridge. The ESI-MS of the reaction mixture that results from refluxing one equivalent of 2,6-isophthaloyl chloride with two equivalents of **1** in acetonitrile solution indicates formation of a single tethered dibenzotetramethyltetraaza[14]annulene derivative (SIT-tmtaa) (**2**) as the major product along with a small amount of a double tethered derivative DIT-tmtaa, (**3**) (Fig. S1). Increasing the ratio of 2,6-isophthaloyl chloride to **1** to a ratio of 1:1 results in an increase in the yield of **3** to approximately 25% in the crude mixture, consistent with the proposed reaction scheme (scheme 1). However, the isolation of this still low-yield product in pure form from the other products was not successful. The ESI-MS

for the mass regions associated with the single- and double-tethered derivatives **2** and **3** are shown in Figs. 2 and 3. The single-tethered derivative **2** was successfully purified by recrystallization from acetonitrile. The UV-visible spectra of **1** and **2** in benzene are shown in Fig. S2. The λ_{max} for the $\pi-\pi^*$ transition of **2** (341 nm) shows only a 6 nm blue shift from the corresponding value for **1** (347 nm) which indicates that the carbonyl functionality of the tethering group does not strongly perturb the electronic structure of the macrocycle.

Scheme 1: Synthesis of single- and double-tethered tmtaa dimers

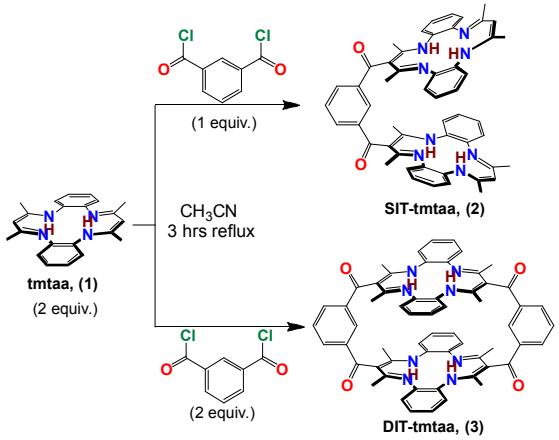

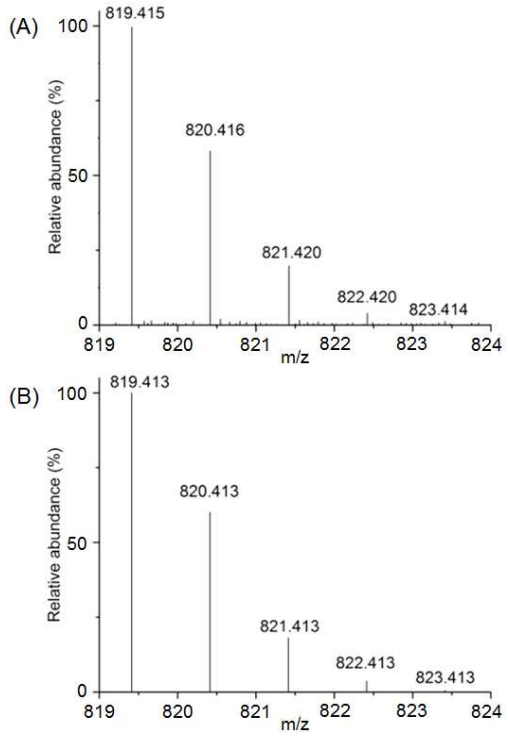

Fig. 2 (A) Experimental and (B) theoretical isotopic distribution pattern in ESI-MS of $[M+1]^+$ of $\mathbf{2}^+$.

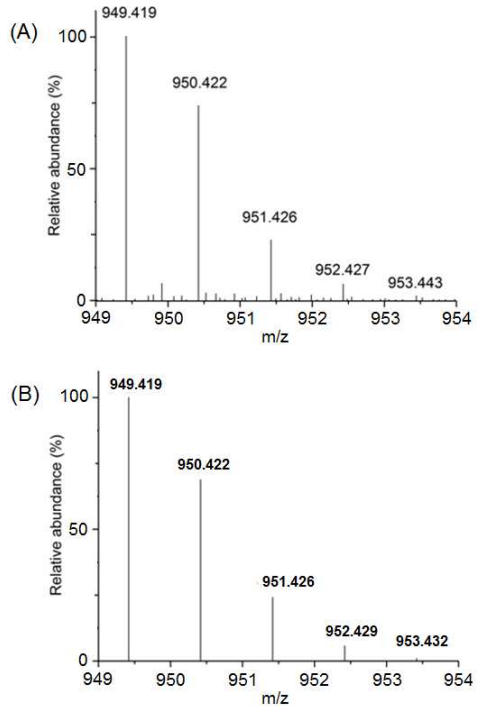

Fig. 3 (A) Experimental and (B) theoretical isotopic distribution pattern in ESI-MS of $[M+1]^+$ peak of $\mathbf{3}^+$.

2. Single Crystal X-Ray Structural Characterization of The Tethered Compound 2:

The single-tethered free base compound **2** crystallizes in a triclinic crystal system in the $P\bar{1}$ space group. Table S1 gives the crystal data and data collection parameters for **2** and selected bond distances and angles are given in Table S2. Fig. S3 in the displays molecular packing diagram of **2** in the crystal lattice. Fig. 4 displays the perspective views of **2**, that show a syn orientation of the tethered tetramethyltetraaza[14]annulene macrocycles. The average Ct_{14}•••N (Ct_{14} = center calculated taking all [14]anulene ring atoms) and Ct_{N4}•••N (Ct_{N4} = center calculated taking only four 'N' ring atoms) distances for **2** are decreased to 1.904 Å (ring-I), 1.900 Å (ring-II) and 1.871 Å (ring-I), 1.880 Å (ring-II), respectively, from 1.921 Å and 1.904 Å, respectively, obtained for untethered **1** (Table 1). The Ct_{14}•••Ct_{14} and Ct_{N4}•••Ct_{N4} distances are found to be 7.481 and 7.034 Å, respectively. The ring deformations are best appreciated by the out of mean plane displacements (in units of 0.01 Å) of 14 ring atoms from the least-squares planes of $C_{10}N_4$ [14]annulene core atoms and four 'N' ring atoms for **1** and **2** (Figs. 5 and S4, Table 1), which indicate that the tetraaza[14]annulene macrocycles are more distorted from planarity in case of the tethered compound **2** compared to the parent tmtaa (**1**). The inter-planar angle between two least-squares planes of the $C_{10}N_4$ [14]annulene core atoms and four 'N' ring atoms of two tmtaa units (88.33° and 86.51°, respectively) indicates a near orthogonal orientation of the two macrocyclic units in spite of their syn-like arrangement.

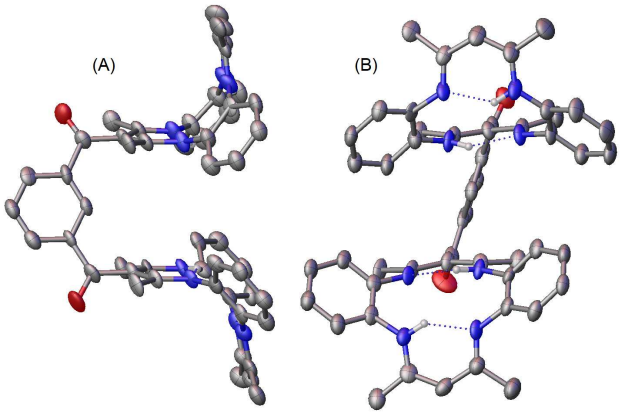

Fig. 4 Perspective (A) side and (B) front views of **2** showing 50% thermal contours for all non-hydrogen atoms at 100 K (C-H hydrogen atoms and n-pentane have been omitted for clarity).

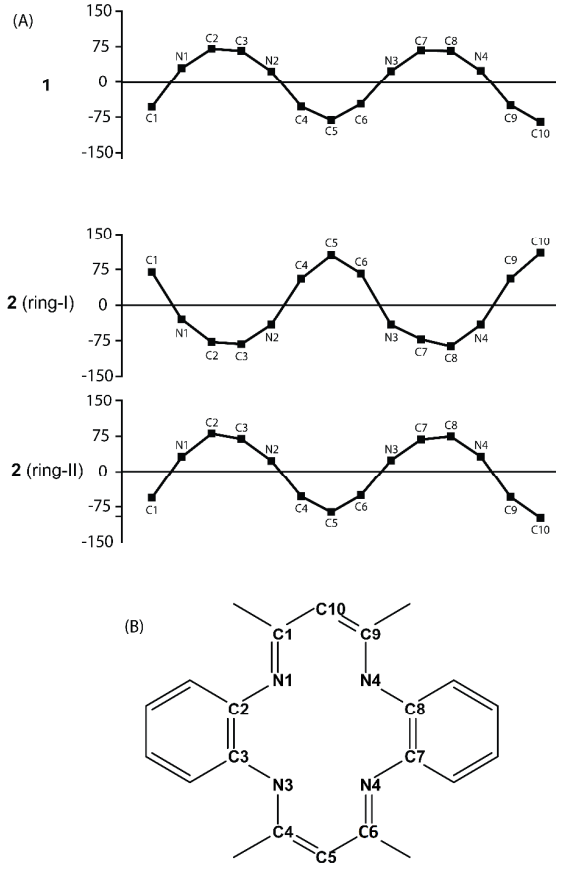

Fig. 5 (A) Out-of-plane displacements (in unit of 0.01 Å) of [14]annulene core atoms of **1** and **2** from least-squares planes of $C_{10}N_4$ ring atoms. The horizontal axes denote the bond connectivity between atoms. (B) The corresponding atom numbers of $C_{10}N_4$ [14]annulene.

Table 1. Selected Structural and Geometrical Parameters

Compound		Ct_{14}•••N (Å)	Δ_{14}[a] (Å)	Θ_1[b] (°)	Ct_{N4}•••N (Å)	Δ_{N4}[c] (Å)	Θ_2[d] (°)
1[e]		1.921	0.49	NA	1.904	0.02	NA
2	ring-I[f]	1.904	0.62	88.33	1.871	0.06	86.5
	ring-II[f]	1.900	0.54		1.880	0.01	1

[a] average deviation of 14 anulene ring atoms from least-squares plane of the $C_{10}N_4$ core atoms. [b] Inter-planar angle between two least-squares planes of the $C_{10}N_4$ core atoms. [c] Average deviation of four 'N' ring atoms from least-squares plane of four 'N' ring atoms. [d] Inter-planar angle between two least-squares planes of four 'N' ring atoms. [e] Structure taken from Ref. 12. [f] Ring-I and ring-II refers to two separate [14]anulene rings.

3. ^{1}H NMR of 2:

^{1}H NMR spectra for 2,6-isophthaloyl chloride, tmtaa (**1**) and the SIT-tmtaa (**2**) in $CDCl_3$ at 295 K are given in Fig. 6. The ^{1}H NMR for the macrocycle in **2** shows one methine hydrogen resonance with a relative area of 1, two NH peaks each with area of 2, two methyl resonances each of area 6 and an ABCD aryl hydrogen pattern that reflect substitution of a 2,6-isophthaloyl group for one of the methine hydrogens in **1**. The pattern of 2, 6-isophthaloyl resonances for **2** is the same as that for 2,6-isophthaloyl chloride, which demonstrates that two macrocycle units are attached to 2,6-isophthaloyl bridging group. The ^{13}C NMR spectrum is also consistent with the symmetry of **2**, showing the appropriate number of carbonyl, methyl, and TMTAA-based peaks, though two of the aryl ^{13}C peaks overlap (Fig S5).

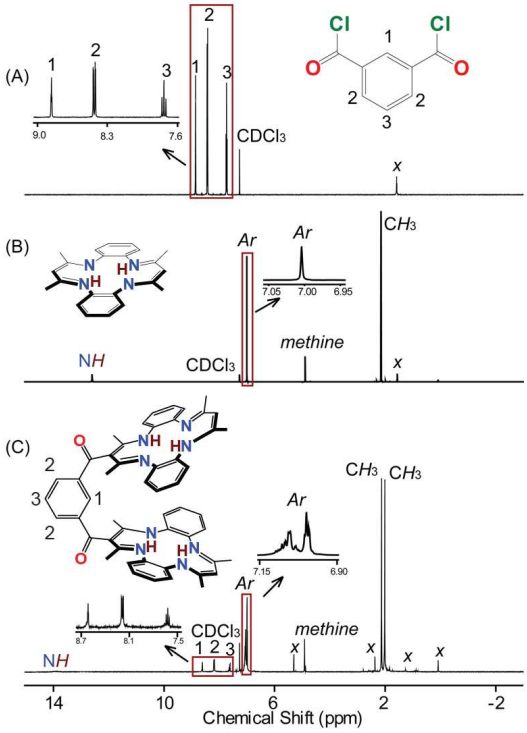

Fig. 6 500 MHz ^{1}HNMR spectra in $CDCl_3$ (at 295 K) of (A) 2, 6-isophthaloyl chloride, (B) **1** and (C) **2**. 'x' represent impurities.

4. Di-nickel(II) complex of 2:

The di-nickel(II) complex of **2** is readily generated by mixing a benzene solution of **2** with nickel(II) acetate in acetonitrile. Successful di-nickellation is confirmed by mass spectrometry (m/z 931.2527 (M^+, 100%). Theor: 931.2529). Numerous attempts at crystallization from benzene, chloroform and acetonitrile did not produce X-ray quality single crystals of the di-nickel(II) complex of **2**. The UV-visible spectra of the di-nickel(II) complex of **2** and (tmtaa)Ni(II) (**1-Ni**) in benzene are nearly super imposable which shows that the intra-macrocycle interactions are small (Fig. 7). The ^{1}H NMR spectra for C_6D_6 solutions of (tmtaa)Ni(II), **1-Ni**, and the di-nickel(II) complex of **2, 2-Ni**, are shown in Fig. 8. The regions of primary importance are shown in expanded inserts designated by arrows. Coordination of Ni(II) by both of the tethered tmtaa units is shown by the complete disappearance of the N-H resonances, equivalence of the tethered tmaa units and a symmetrical 2,6-isophthaloyl bridge. ^{13}C NMR gives the appropriate number of individual ^{13}C signals and is consistent with the symmetry of the tethered ligand (Fig. S6).

Scheme 2: Synthesis of single tethered nickel(II) tmtaa dimer

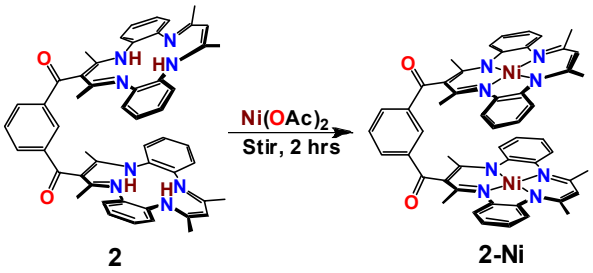

Chart 1

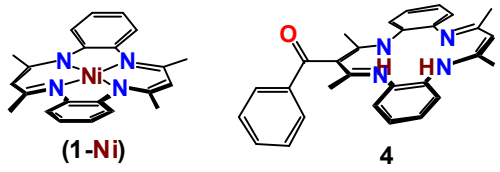

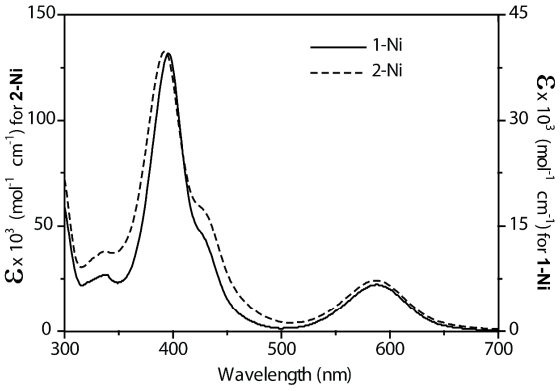

Fig. 7. UV-visible spectra of 6.1 × 10^{-6} (M) **1-Ni** and 4.8 × 10^{-6} (M) **2-Ni** in benzene at 295 K.

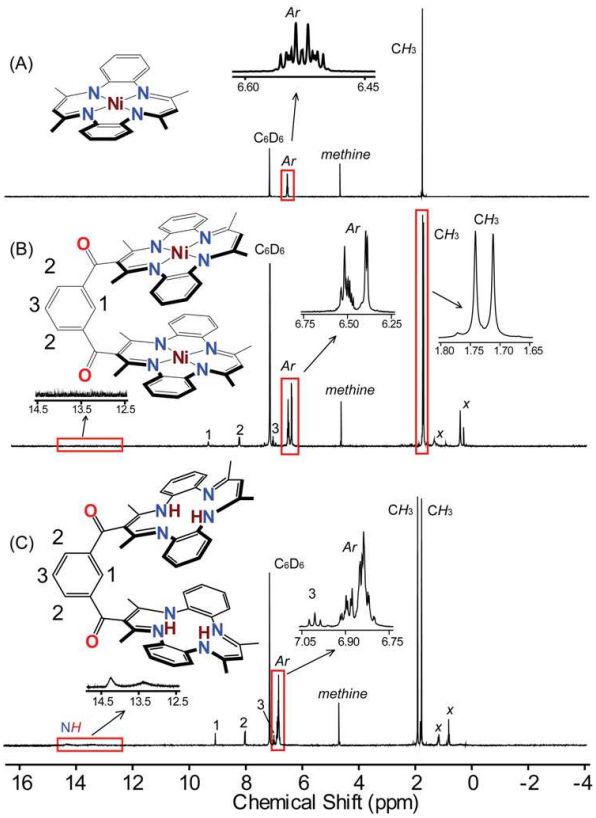

Fig. 8 500 MHz ^{1}HNMR spectra in C_6D_6 (at 295 K) of (A) **1-Na**, (B) **2-Ni** and (C) **2**. '*x*' represent impurities.

5. DFT Calculations:

The DFT optimized geometry of **2** (Fig. S7) at the B3LYP/6-31G level provides a close agreement with the single crystal X-ray structure demonstrating just 6.16° and 0.92° differences for interplanar angles Θ1 and Θ2, respectively. Fig. S8 displays electronic distribution in some selected molecular orbitals of **1**, **2, 3** and **4** (Chart 1) obtained by performing similar DFT calculations. The HOMO of all four molecules resides on tmtaa units. However the LUMO of **2**, **3** and **4** reside on the 2, 6-isophthaloyl bridge, in contrast to that of **1**. In addition, HOMO-1, LUMO+2 and HOMO, LUMO+3 of **2** are residing on two separate [14]annulene units. On the other hand, LUMO+2, LUMO+3, LUMO+4 and LUMO+5 of **3** delocalized between the bridge and [14]anulene units. The HOMOs and LUMOs of **1** and **2** are displayed in Fig 9 as representative displaying significant role of the bridging unit on the electronic structure of **2**.

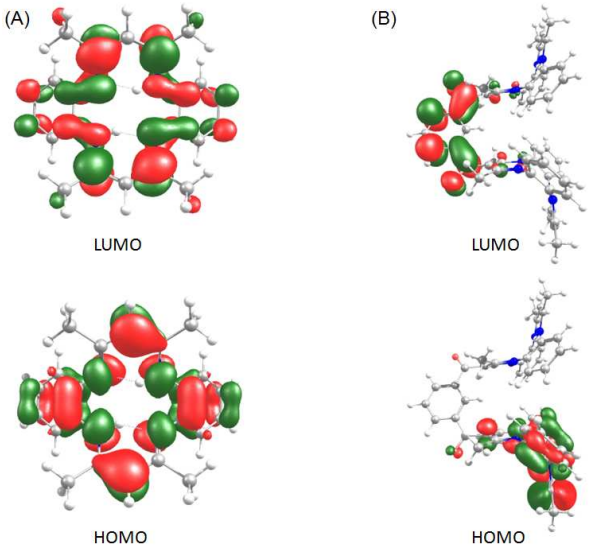

Figure 9 HOMO and LUMO of (A) **1** and (B) **2** calculated by using DFT at B3LYP/6-31G level.

In the absence of a single crystal X-ray structure, we have optimized the geometry of **2-Ni** at the B3LYP/3-21G level and the perspective views (side and front views) of the complex along with some structural parameters are shown in Fig 10. Two tmtaa units retains their syn like orientation with relatively lower interplanar angles (47.01° and 47.12°) between the least square planes of $C_{10}N_4$ core atoms (Θ1) and four ring 'N' atoms (Θ2), respectively, in comparison to the corresponding free ligand (Θ1=82.17° and Θ2=85.59°, obtained from optimized geometry of **2**). The Ni•••Ni distance is found to be 6.474 Å. These geometrical parameters clearly points towards the pacman type vertical flexibility of the spacer.[13] All the optimized geometries and their corresponding cartesian coordinates are given in the supporting information.

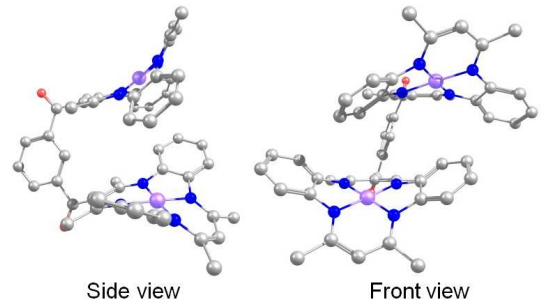

$Ni–N_{eq}$ = 1.822 (ring-I) and 1.822 (ring -II)
Δ_{14}^{Ni} = 0.136 (ring-I) and 0.135 (ring-II)
Δ_{N4}^{Ni} = 0.009 (ring-I) and 0.008 (ring-II)
Ni•••Ni = 6.474
Θ1 = 47.01° and Θ2 = 47.12°

Fig. 10 B3LYP optimized structure of **2-Ni** (with bond lengths and distances are given in Angstroms), as calculated using the 3-21G basis set for all atoms.

Electrochemistry

Electrochemical measurements on **2** and **2-Ni**were performed to examine redox properties of these molecules. Both molecules exhibit a single irreversible oxidation wave, and no visible reduction waves within the potential window of solvent acetonitrile (Fig. 11). The oxidation of the ligand at the electrode results in compound decomposition in both cases as evidence by the irreversibility of the wave, as well as by repeat scans which shows that the intensity of the wave decreases with increasing scan number due to depletion of the concentration of the molecule near the electrode surface following decomposition (SI). The measured potential for this redox event in the nickel complex is lower than that of the unmetallated ligand due to the increased negative charge on the ligand in the Ni complex with the dianionic ligand in comparison to the neutral protonated **2**. In the case of **2-Ni**, the full scan shows the presence of a second wave at 0.9 V vs. Fc, however this second wave is assigned to the decomposition product of **2-Ni** based on its persistence during repeat scans, while the wave at 0.23 V shown in Figure 11 disappears upon repeat scans (See SI). These results suggest that the first oxidation event in **2-Ni** triggers a decomposition, and that the decomposition product has a redox event at 0.9 V that is quasi-reversible.

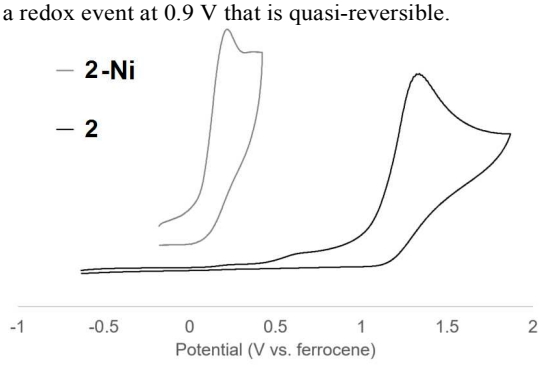

Fig. 11. Cyclic voltammagrams of **2** and **2-Ni** vs Fc/Fc^+ in acetonitrile solvent.

These oxidation events are ligand based, necessarily for **2**, being the unmetallated complex, and based on the calculated HOMO orbital of **2** (Figure 9), which shows that the HOMO is based in the TMTAA π-system for **2** (Figure 9), and the disruption of the π-electron system by oxidation at an electrode triggers molecular decomposition in both cases.

Conclusions

Selective reaction of acid chlorides with the methine hydrogen of tmtaa to introduce acyl groups is applied in tethering two tetraaza[14]annulene (tmtaa) macrocycles by reactions of a bi-functionalized di-acid chloride, 2,6-isophthaloyl chloride. The resulting single 2,6-isophthaloyl tethered di-tmtaa (SIT-tmtaa, **2**) is the first reported structurally characterized covalently tethered di-tetraaza[14]annulene species. The electronic spectrum of **2** shows only a small change in the λ_{max} for the π–π* transition of the untethered tmtaa which indicates that the carbonyl units in the bridging group do not substantially alter

the tmtaa electronic structure. Interactions with the specific 2,6-isophthaloyl group cause the tethered tmtaa macrocycles to deviate more from planarity than that which occurs in the untethered tmtaa. DFT computations suggest that the 2,6-isophthaloyl tether provides a level of flexibility in the inter tmtaa distances that is comparable to the Pacman Effect observed for tethered porphyrins.

The di-acid chloride tethering method has substantial potential for varying the structures for bridging units for tetraaza[14]annulene macrocycles and also for tethering a wide range of macrocycles and multidentate ligands that have reactive methine type hydrogens. The synthetic versatility and simplicity of this approach suggests application in the design of selective molecular tweezers.[7] Multiply-bridged species are accessible from ligands that have more than one reactive methine hydrogen. Tetraaza[14]annulene macrocycles like tmtaa have two reactive methine hydrogens that can give double-tethered species and porphyrins can have as many as four methine hydrogens for use in tethering. The synthetic versatility and simplicity of this approach suggests application in the design of molecular tweezer type materials for selective muti-centered binding and reactivity. The scope of tethering groups from diacid chlorides and the range of multidentate ligands that can be tethered by this method are currently being evaluated.

Experimemtal Section

1. General

Reagents were purchased from commercial sources (Aldrich, Strem). Anhydrous solvents such as acetonitrile, chloroform, benzene, and *n*-pentane were purified using an Innovative Technology, Inc. Pure Solv system. Solvents were stored in a glove-box over activated molecular sieves for at least 8 h prior to use. ^{1}H NMR spectra were recorded on a Bruker Avance 500 MHz spectrometer. Values for chemical shifts (ppm) are referenced to the residual protio-solvent resonances (C_6D_6 7.16 ppm and $CDCl_3$ 7.26 ppm). Accurate mass measurement analyses were conducted on a Waters LCT Premier XE, time-of-flight, LCMS with electrospray ionization (ESI). Samples were taken up in a suitable solvent for analysis. The signals were mass measured against an internal lock mass reference of leucine enkephalin. Waters software calibrates the instruments, and reports measurements, by use of neutral atomic masses. The mass of the electron is not included. Electrochemical measurements were performed on a CH electrochemical apparatus using a three-electrode setup: A glassy carbon working electrode, a platinum counter electrode, and a AgCl(s) coated Ag/AgCl reference electrode. Electrochemical measurements were performed in a 0.1 M solution of tetrabutylammonium perchlorate in acetonitrile. The CV wave of ferrocene in acetonitrile was measured to convert the voltage axis to the ferrocene/ferrocenium reference electrode.

2. X-ray Diffraction

X-ray data were collected on a Bruker KAPPA APEX II DUO diffractometer. Single crystals were mounted on a MiTeGen loop using paratone-N oil. Single crystal data were obtained using Mo Kα radiation from a sealed tube equipped with a TRIUMPH monochromator, and processed using the APEX2 software suite. Structures were solved using direct methods and refined using full-matrix least-squares minimization using the SHELX crystallography package[14] with OLEX2 as a GUI and graphics program.[15]

3. Density Functional Theory

Geometry optimization of **1** and **2** were initiated from the crystal structure coordinates. All structure optimizations were carried out by employing a B3LYP hybrid functional, using the Gaussian 09 package.[16] The method used was Becke's three-parameter hybrid exchange functional provided by the Lee, Yang, and Parr expression for the nonlocal correlation,[17] and the Vosko, Wilk, and Nussair 1980 correlation functional (III) for local correction.[18] The basis set was set as 3-21G in case of Ni derivative and 6-31G for all the other molecules for all atoms.

4. Preparations

1 has been synthesized based on the procedures reported in literature.[18]

Preparation of 2**:** 2, 6-isophthaloyl chloride (17 mg, 0.084 mmol), dissolved in dry CH_3CN (20 mL), was added drop-wise over a period of 30 minutes to 1 (116 mg, 0.337 mmol) in dry CH_3CN (100 mL) under N_2 atmosphere. The mixture was then refluxed for additional 3 hrs under nitrogen. The reaction mixture was filtered while hot to remove any solid particles, and the filtrate was kept at 4° C for 12 hrs. The solid precipitate was collected by filtration and washed with cold CH_3CN several times to obtain ~95% purity **2** (Yield 34 mg, 50%) based on ^{1}H NMR. UV-visible (C_6H_6) [λ_{max}, nm (ε, M^{-1} cm^{-1})]: 341 (1.05×10^5). ^{1}H NMR (C_6D_6, 295 K): -N*H*: 14.25 (2H, bs) and 13.38 (2H, bs); isophthaloyl: 9.06 (1H, s), 8.02 (2H, d) and 7.01 (1H, t); benzyl: 6.95-6.77 (16H, m), methine-*H*: 4.73 (2H, s); -CH_3: 1.98 (12H, s) and 1.84 (12H, s). ($CDCl_3$, 295 K): -N*H*: 13.95 (2H, bs) and 13.38 (2H, bs); isophthaloyl: 8.61 (1H, s), 8.19 (2H, d) and 7.62 (1H, t); Ar: 7.15-6.92 (m), methine-*H*: 4.91 (2H, s); -CH_3: 2.13 (12H, s) and 2.01 (12H, s). ^{13}C NMR ($CDCl_3$, 295 K): C=O: 196.81, imine C=N: 160.75, 158.34, aryl *ipso* aryl C: 137.44, 136.33, Aryl methine: 132.13, 132.00, 128.59, 128.02, 123.52, 122.19, 121.98, annulene CO-substitued methine: 107.55, annulene C-H methine: 97.05, methyl: 19.44, 18.94. Two of the aryl peaks are presumed to overlap. ESI-MS: m/z 819.4163 ($[M+1]^+$, 100%). Theor: 819.4135

Preparation of 3: 2, 6-isophthaloyl chloride (64 mg, 0.315 mmol) dissolved in dry CH_3CN was added drop-wise over a period of 30 minutes to **1** (116 mg, 0.337 mmol) in dry CH_3CN (100 mL) under N_2 atmosphere. The mixture was then refluxed for additional 3 hrs under nitrogen. The reaction mixture was filtered while hot to remove any solid particles, and the filtrate

was kept at 4°C for 12 hrs. The solid precipitate obtained was collected by filtration and washed with cold CH_3CN for several times to obtain product that have ~25% of **3** based on ^1H NMR. ESI-MS: m/z 949.419 ($[M+1]^+$, 100%). Theor: 949.419

Preparation of the di-nickel(II) complex of 2 (2-Ni): **2** (50 mg, 0.061 mmol) was dissolved in 50 mL of dry C_6H_6 in a two-necked round bottom flask. The solution was stirred under a nitrogen atmosphere. When a clear solution was formed, 5 mL saturated solution of $Ni(OAc)_2$ in CH_3CN was added and stirring was continued for another 3 hrs, while the colour changed to green from yellow. The resulting solution was dried completely and washed with CH_3CN to obtain dark green solid of **2-Ni**. (Yield 40 mg, 75%). UV-visible (C_6H_6) [λ_{max}, nm (ε, M^{-1} cm^{-1})]: 391 (1.33×10^5), 585 (2.41×10^4). ^1H NMR (C_6D_6, 295 K): isophthaloyl: 9.34 (1H, s), 8.24 (2H, d) and 7.06 (1H, t); Ar: 6.58-6.37 (16H, m), methine-*H*: 4.64 (2H, s); -C*H*$_3$: 1.74 (12H, s) and 1.71 (12H, s). ^{13}C NMR ($CDCl_3$, 295 K): C=O: 196.46, imine C=N: 155.50, 154.24, benzo *ipso* C: 148.12, 147.91, isophthalolyl: 141.09, 136.13, 134.07, 130.05, benzo methane: 123.19, 122.43, 122.07, 121.19, annulene CO-substituted methine: 119.93, annulene methine: 111.91, methyl. 21.72, 20.64. ESI-MS: m/z 931.2527 (M^+, 100%). Theor: 931.2529.

Preparation of Nickel(II) complex of 1 (1-Ni): (tmtaa)Ni(II) was synthesized by following reported procedures.[19]

Conflicts of interest

There are no conflicts to declare.

Acknowledgements

The authors gratefully acknowledge support of this research through NSF Grant 1362016 and the Temple University College of Science and Technology. Support for the NMR facility at Temple University by a CURE grant from the Pennsylvania Department of Health is gratefully acknowledged. We thank Dr. Charles W. Ross III, Director: Automated Synthesis and Characterization of the University of Pennsylvania Chemistry Department for providing mass spectral analyses, and data interpretation.

References

1 (a) M. Beller and C. Bolm, *Transition Metals for Organic Synthesis, ed. Wiley-VCH, Weinheim, Germany,* 2004, vol. **2**. (b) F. Diederich, P. J. Stang and R. R. Tykwinski, *Acetylene Chemistry: Chemistry, Biology and Material Science, ed. Wiley-VCH, Weinheim, Germany,* 2005. (c) B. M. Trost and C. -J. Li, *Modern Alkyne Chemistry: Catalytic and Atom-Economic Transformation, ed. Wiley-VCH, Weinheim, Germany,* 2015.

2 (a) K. M. Zwoliński, L. Sieroń and J. Eilmes, *Org. Chem. Front* 2018, **5**, 171. (b) J. A. Paquette and J. B. Gilroy, *J. Polym. Sci. A*, 2016, **54**, 3257.

3 (a) J. L. Sessler, E. Karnas and E. Sedenberg, *Porphyrins and Expanded Porphyrins as Receptors, in Supramolecular Chemistry: From Molecules to Nanomaterials, ed.* J. W. Steed and P. A. Gale, *John Wiley & Sons, Chichester, UK,* 2012, 1045. (b) H. L. Anderson, S. Anderson and J. K. M. Sanders, *J. Chem. Soc., Perkin Trans.*, 1995, **1**, 2231. (c) K. -I. Sakaguchi, T. Kamimura, H. Uno, S. Mori, S. Ozako, H. Nobukuni, M. Ishida and F. Tani, *J. Org. Chem.,* 2014, **79**, 2980. (d) A. Ouchi, K. Tashiro, K. Yamaguchi, T. Tsuchiya, T. Akasaka and T. Aida, *Angew. Chem., Int. Ed.,* 2006, **45**, 3542.

4 N. Aratani, D. Kim and A. Osuka, *Acc. Chem. Res.,* 2009, **42**, 1922.

5 (a) R. P. Bonar-Law, L. G. Mackay, C. J. Walter, V. Marvaud, J. K. M. Sanders, *Pure Appl. Chem.,* 1994, **66**, 803. (b) L. G. Mackay, R. S. Wylie, J. K. M. Sanders, *J. Am. Chem. Soc.*, 1994, **116**, 3141.

6 (a) S. Li, W. Cui and B. B. Wayland, *Chem. Commun.*, 2007, 4024. (b) W. Cui, X. P. Zhang and B. B. Wayland, *J. Am. Chem. Soc.* 2003, **125**, 4994. (c) X. -X. Zhang and B. B. Wayland, *Inorg. Chem.* 2000, **39**, 5318. (d) X. -X. Zhang, G. F. Parks and B. B. Wayland, *J. Am. Chem. Soc.* 1997, **119**, 7938. (e) X. -X. Zhang and B. B. Wayland, *J. Am. Chem. Soc.* 1994, **116**, 7897.

7 (a) J. Leblond and A. Petitjean, ChemPhysChem 2011, **12**, 1043. (b) F.-G. KläRner and B. Kahlert, Acc. Chem. Res. 2003, **36**, 919.

8 (a) O. Horváth, Z. Valicsek, M. A. Fodor, M. M. Major, M. Imran, G. Grampp and A. Wankmüller, *Coord. Chem. Rev.*, 2016, **325**, 59. (b) T. Haino, *Chem. Rec.*, 2015, **15**, 837. (c) D. Margetić, *Current Organic Chemistry,* 2012, **16**, 829. (d) P. D. Harvey, C. Stern, C. P. Gros and R. Guilard, *J. Porphyrins Phthalocyanines*, 2010, **14**, 55.

9 (a) R. Inoue, S Kawamorita, T. Naota. *Chem. Eur. J.*, 2016, **22**, 5712–5726. (b) N. Komiya, T. Muraoka, M. Iida, M. Miyanaga, K. Takahashi, T. Naota. *J. Am. Chem. Soc.,* 2011, **133**, 16054-16061.

10 (a) G. H. Imler, G. M. Peters, M. J. Zdilla and B. B. Wayland, *Inorg. Chem.*, 2015, **54**, 273. (b) G. H. Imler, G. M. Peters, M. J. Zdilla and B. B. Wayland, *J. Am. Chem. Soc.*, 2014, **136**, 5856. (c) G. H. Imler, M. J. Zdilla and B. B. Wayland, *Inorg. Chem.*, 2013, **52**, 273.

11 K. Sakata, H. Tagami and M. Hashimoto, *J. Heterocycl. Chem.,* 1989, **26**, 805.

12 V. L. Goedken, J. J. Pluth, S. -M. Peng and B. Bursten, *J. Am. Chem. Soc.*, 1976, **98**, 8014.

13 (a) P. Lang and M. Schwalbe, *Chem. Eur. J.* 2017, **23**, 17398. (b) C. J. Chang, Z.-H. Loh, Y. Deng and D. G. Nocera, Inorg. Chem. 2003, **42**, 8262.

14 G. M. Sheldrick, Acta Crystallogr., Sect. A: Found. *Crystallogr.*, 2008, **A64**, 112.

15 O. V. Dolomanov, L. J. Bourhis, R. J. Gildea, J. A. K. Howard and H. Puschmann, *J. Appl. Crystallogr.* 2009, **42**, 339.

16 M. J. Frisch, G. W. Trucks, H. B. Schlegel, G. E. Scuseria, M. A. Robb, J. R. Cheeseman, G. Scalmani, V. Barone, B. Mennucci, G. A. Petersson, H. Nakatsuji, M. Caricato, X. Li, H. P. Hratchian, A. F. Izmaylov, J. Bloino, G. Zheng, J. L. Sonnenberg, M. Hada, M. Ehara, K. Toyota, R. Fukuda, J. Hasegawa, M. Ishida, T. Nakajima, Y. Honda, O. Kitao, H. Nakai, T. Vreven, J. A. Montgomery, Jr., J. E. Peralta, F. Ogliaro, M. Bearpark, J. J. Heyd, E. Brothers, K. N. Kudin, V. N. Staroverov, R. Kobayashi, J. Normand, K. Raghavachari, A. Rendell, J. C. Burant, S. S. Iyengar, J. Tomasi, M. Cossi, N. Rega, J. M. Millam, M. Klene, J. E. Knox, J. B. Cross, V. Bakken, C. Adamo, J. Jaramillo, R. Gomperts, R. E. Stratmann, O. Yazyev, A. J. Austin, R. Cammi, C. Pomelli, J. W. Ochterski, R. L. Martin, K. Morokuma, V. G. Zakrzewski, G. A. Voth, P. Salvador, J. J. Dannenberg, S. Dapprich, A. D. Daniels, Ö. Farkas, J. B. Foresman, J. V. Ortiz, J. Cioslowski and D. J. Fox, Gaussian, Inc., Wallingford CT, 2009.

17 (a) A. D. Becke, *J. Chem. Phys*., 1993, **98**, 5648. (b) C. Lee, W. Yang and R. G. Parr, *Phys. Rev. B: Condens. Matter Mater. Phys*., 1988, **37**, 785.
18 (a) S. H. Vosko, L. Wilk and M. Nusair, *Can. J. Phys.*, 1980, **58**, 1200. (b) S. H. Vosko and L. Wilk, *Phys. Rev. B: Condens. Matter Mater. Phys*., 1980, **22**, 3812.
19 J. H. Niewahner, K. A. Walters and A. Wagner, *J. Chem. Educ.*, 2007, **84**, 477.